Proximal Cavity, Distal Histidine, and Substrate Hydrogen-Bonding Mutations Modulate the Activity of *Amphitrite ornata* Dehaloperoxidase†

Stefan Franzen,*,‡ Jennifer Belyea,‡ Lauren B. Gilvey,‡ Michael F. Davis,‡ Chelsea E. Chaudhary,‡ Tim L. Sit,§ and Steven A. Lommel§

Departments of Chemistry and Plant Pathology, North Carolina State University, Raleigh, North Carolina 27695

Received January 5, 2006; Revised Manuscript Received May 31, 2006

ABSTRACT: Dehaloperoxidase (DHP) from *Amphitrite ornata* is the first globin that has peroxidase activity that approaches that of heme peroxidases. The substrates 2,4,6-tribromophenol (TBP) and 2,4,6-trichlorophenol are oxidatively dehalogenated by DHP to form 2,6-dibromo-1,4-benzoquinone and 2,6-dichloro-1,4-benzoquinone, respectively. There is a well-defined internal substrate-binding site above the heme, a feature not observed in other globins or peroxidases. Given that other known heme peroxidases act on the substrate at the heme edge there is great interest in understanding the possible modes of substrate binding in DHP. Stopped-flow studies (Belyea, J., Gilvey, L. B., Davis, M. F., Godek, M., Sit, T. L., Lommel, S. A., and Franzen, S. (2005) *Biochemistry 44*, 15637−15644) show that substrate binding must precede the addition of H_2O_2. This observation suggests that the mechanism of DHP relies on H_2O_2 activation steps unlike those of other known peroxidases. In this study, the roles of the distal histidine (H55) and proximal histidine (H89) were probed by the creation of site-specific mutations H55R, H55V, H55V/V59H, and H89G. Of these mutants, only H55R shows significant enzymatic activity. H55R is 1 order of magnitude less active than wild-type DHP and has comparable activity to sperm whale myoglobin. The role of tyrosine 38 (Y38), which hydrogen bonds to the hydroxyl group of the substrate, was probed by the mutation Y38F. Surprisingly, abolishing this hydrogen bond increases the activity of the enzyme for the substrate TBP. However, it may open a pathway for the escape of the one-electron product, the phenoxy radical leading to polymeric products.

The enzyme dehaloperoxidase (DHP[1]), first isolated from the terebellid polychaete *Amphitrite ornata*, presents a unique opportunity to study peroxide function in an enzyme that possesses the globin fold (*2*−*4*). The similarity of DHP and sperm whale myoglobin (SWMb) structures is shown in Figure 1A. Although the overall disposition of the key α-helices (B, C, D, E, and F) is nearly identical in the two structures, there is an overall shift of the amino acid structure of DHP by 1.5 Å relative to SWMb when the heme prosthetic group is used to perform a structural superposition. Consequently, the heme of DHP is sequestered 1.5 Å more deeply in the globin than the hemes in typical myoglobins.

Although globins and peroxidases have little structural or sequence similarities, they both typically have a proximal and a distal histidine. The proximal histidine is ligated to the heme iron at Nϵ, and the iron ligation strength is controlled by the hydrogen bond configuration at Nδ-H. The proximal histidine bond to iron is stronger in peroxidases than in globins (*5*, *6*). The strong proximal histidine ligation in peroxidases gives rise to a push that helps to activate the bound peroxide for heterolytic bond cleavage to form the

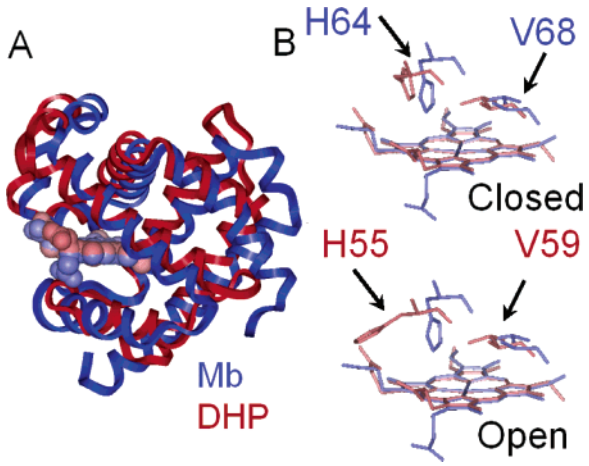

FIGURE 1: Superposition of the DHP and Mb structures using the heme ring atoms as the common atoms. A high-resolution SWMb X-ray structure (*69*) and the DHP structure 1EW6 (*4*) were retrieved from the Protein Data Bank. The superposition was carried out using Insight II (Accelrys, Inc.). (A) Similarity of the helical structure of DHP and SWMb with an offset of 1.5 Å relative to the heme ring atoms. (B) Similarity of the residues in the distal pocket. In the closed conformation, both the valine and histidine are present in the same relative orientation; however, the corresponding residues SWMb-H64/DHP-H55 and SWMb-V68/DHP-V59 are shifted by 1.5 Å relative to the heme iron. The open conformation is also recorded in the DHP X-ray crystal structure (1EW6), which has two sets of coordinates for H55.

† This project was supported by NSF Grant MCB-9874895.

* To whom correspondence should be addressed. Phone: 919-515-8915. Fax: 919-515-8920. Email: Stefan_Franzen@ncsu.edu.

‡ Department of Chemistry.

§ Department of Plant Pathology.

[1] Abbreviations: CcP, cytochrome *c* peroxidase; DBQ, 2,6-dibromo-1,4-benzoquinone; DCQ, 2,6-dichloro-1,4-benzoquinone; DHP, dehaloperoxidase; HRP, horseradish peroxidase; LiP, lignin peroxidase; $P450_{cam}$, cytochrome P450 camphor; TBP, 2,4,6 tribromophenol; TCP, 2,4,6 trichlorophenol; Mb, myoglobin; SWMb, sperm whale myoglobin.

10.1021/bi060020z CCC: $33.50
Published on Web 07/07/2006

reactive species compound I (*7*). The Nϵ-H of the distal histidine in myoglobin (Mb) is ~4.5 Å from the heme iron and plays an important role in stabilizing the oxygen relative to carbon monoxide binding by means of a hydrogen-bonding interaction with bound diatomic ligands (*8*, *9*). The Nϵ-H of the distal histidine in peroxidases is located at a slightly greater distance of ~6.0 Å from the heme iron (*10*−*12*). This location is key to peroxidase function, giving rise to the pull that provides the needed acid−base catalysis for the activation of bound H_2O_2 to form the reactive species compound I in peroxidases (*13*−*16*). These functions have been probed using mutagenesis in globins (*17*−*19*) and peroxidases (*20*−*26*). It is remarkable that the 1.5 Å shift in the DHP protein structure relative to the heme (Figure 1B) places the distal histidine H55 at a distance more appropriate for peroxidase function. However, the consequence of the shift also places the valine V59 closer to the heme iron, and makes it the closest amino acid residue. This structural change has an effect on hydrogen bonding to bound CO (*27*) and NO rebinding dynamics (*28*) that resemble the effect of the H64V mutant of Mb (*8*, *9*, *29*). Furthermore, Figure 1B shows that there are two conformations of H55 in DHP. The open conformation resembles the open conformation of Mb, in which H64 is swung out into a solvent-exposed conformation (*30*). Moreover, the open conformation is required for substrate binding in DHP as shown by an X-ray crystal struture (1EWA) (*3*, *4*).

DHP is unique among globins and peroxidases in that it has an internal substrate-binding site that has been characterized by X-ray crystallography (*3*, *4*). The substrate-binding pocket is surrounded largely by hydrophobic residues, including five phenylalanine side chains (F21, F24, F35, F52, and F60) as well as tyrosine Y38. The hydroxyl group of the substrate, 2,4,6-tribromophenol (TBP), acts as a hydrogen bond acceptor for the hydroxyl group of tyrosine Y38. This interaction may be analogous to the hydrogen bond between the amino acid tyrosine Y96 and the hydroxyl group of camphor in cytochrome P450 camphor ($P450_{cam}$), where the hydrogen bond plays a stabilizing role that controls the stereochemistry of hydroxylation (*31*).

In two recent studies, it has been shown that DHP has peroxidase activity intermediate between the activities of SWMb and horseradish peroxidase (HRP) (*1*, *32*). We have further shown that unlike peroxidases there is an obligatory order for the addition of substrate in DHP (*1*). If H_2O_2 is added before the substrate, DHP is observed in the compound II form, but the enzyme is inactive. The current hypothesis is that DHP performs a two-electron oxidation of a substrate bound in an internal binding site so that it cannot activate the substrate starting from the compound II state (*1*). If the substrate is in the binding pocket prior to the entry of H_2O_2, then compounds I and II are formed in succession and can each perform a one-electron oxidation of the substrate to yield the product (*33*). This hypothesis has a number of important ramifications. First, it suggests that any perturbation to binding in the substrate-binding pocket will affect the efficiency of the two-electron mechanism and may lead to either one-electron reactions (to yield a phenoxy radical) or no reaction if the substrate does not bind sufficiently well. Second, the distal histidine, H55, cannot be in the distal pocket when the substrate binds (according to the X-ray crystal structure (*3*, *4*)), and therefore, it must play some other role than the well-established peroxidase pull mechanism (*13*−*15*). Third, the fact that the activation of peroxide does not occur by the standard route leads to the question of the role played by the proximal histidine, H89.

The functions of the proximal and distal histidines have been probed using mutagenesis in globins and peroxidases. The distal histidine has been mutated to glycine, alanine, serine, leucine, valine, and glutamine among other amino acids in Mb (*17*, *34*−*37*) and to leucine, lysine, glutamate, glutamine and arginine in cytochrome *c* peroxidase (CcP) (*20*, *21*, *23*−*26*, *38*). The mutation of the distal histidine to leucine in CcP reduces the activity by 5 orders of magnitude (*39*). In this study, we have chosen to make the mutation of the distal histidine to valine and arginine. The mutation of the distal histidine to valine (H55V) is analogous to the mutant in CcP that inactivates the enzyme. A second mutant (H55R) was created because the positive charge on arginine at pH 7 ensures that it will be in the solvent-exposed conformation. H55R mimics the solvent-exposed or open conformation shown in Figure 1B. Experiments using CO and NO as probes are consistent with a strong interaction by the valine acting as the primary amino acid interacting with bound diatomic ligands (*1*, *27*, *28*). Because V59 is the closest residue to the iron in DHP (Figure 1B), we further probed the effect of the double mutant H55V/V59H, a histidine swap mutant, to determine whether the displacement of histidine would affect DHP function.

The proximal ligand has been mutated to glycine in both Mb (H93G) and CcP (H175G) (*40*−*43*). An exogenous ligand in the so-called proximal cavity mutants can be dialyzed into the proximal pocket to ligate with the heme iron. A range of substituted imidazoles and pyridines have been studied in this manner to systematically change the properties of the heme iron (*44*−*47*). In the present study, the recombinant protein was grown in *E. coli*, and the H89G mutant was expressed in the presence of 10 mM imidazole so that it ligates to the heme iron exactly as was done in H93G Mb (*44*, *45*).

Finally, the stability of the substrate in the binding pocket above the heme was probed by the mutation Y38F, analogous to the mutation Y96F in $P450_{cam}$ (*31*). The resultant mutants were assayed at pH 7 by a time-resolved spectroscopic acquisition of the reaction with native substrate 2,4,6-tribromophenol (TBP) and an analogue, 2,4,6-trichlorophenol (TCP). The similarity of these results to those from analogous mutants of peroxidases demonstrates the functional importance of both the proximal and distal histidines in DHP despite the large structural differences with respect to other known peroxidases.

MATERIALS AND METHODS

Mutagenesis. Generation of DHP Mutants. The cloning of a 6X-His tagged DHP into the pET16b expression plasmid has been described previously (*1*). The Y38F mutant (pET16b-Y38F) was produced by amplifying DHP with primers DHP-5′ 6XHIS and DHP-3′ Y38F (Supporting Information) followed by digestion with *Nco*I/*Sac*I and ligation into a similarly cleaved pET16b-6XHisDHP. Mutants pET16b-H55R, -H55V, -H55V/V59H, and -H89G were produced by site-directed mutagenesis with primers listed in the Supporting Information utilizing the QuikChange II

Table 1: Fits to the Kinetics of the Appearance of the Product at the Maximum Absorbance of the Corresponding 2,6-Dihaloquinone

enzyme	substrate	λ_{max} (nm)	k_{obs}	ΔA
H55R	TBP	290	0.00164	0.016
DHP	TBP	290	0.0130	0.067
			0.00164	0.017
Y38F	TBP	290	0.0535	0.10
H55R	TCP	272	0.0033	−0.0083
DHP	TCP	272	0.00912	−0.23
			0.00033	−0.04
			0.00530	0.135
Y38F	TCP	272	0.0393	−0.17
			0.00278	0.012
			0.00128	0.066

Table 2: Fits to the Kinetics of the Disappearance of the Substrate at the Maximum Absorbance of the Corresponding 2,4,6-Trihalophenol

enzyme	substrate	λ_{max} (nm)	k_{obs}	ΔA
H55R	TBP	316	0.00064	0.036
DHP	TBP	316	0.0136	0.025
			0.00086	0.029
Y38F	TBP	316	0.0630	0.046
			0.00071	0.021
H55R	TCP	316	0.00061	0.073
DHP	TCP	316	0.00886	0.058
			0.00125	0.0010
			0.00483	−0.037
Y38F	TCP	316	0.0416	0.053
			0.00160	0.032
			0.00200	−0.039

Site-Directed Mutagenesis kit (Stratagene, La Jolla, CA). All mutations were verified by sequence analysis.

The recombinant DHP proteins were purified from *E. coli* following previous procedures (*1*).

Assays. A Hewlett-Packard 8453 multiwavelength spectrophotometer was used to obtain the relative activities of wild-type and mutant DHPs. Substrate TBP and the analogue TCP were obtained from Acros Organics. The samples were prepared in 100 mM potassium phosphate buffer at pH 7 with a DHP and mutant concentration ranging from 0.5 to 3.0 μM and an H_2O_2 concentration of 50 μM. The concentration of the substrate was 156 μM.

The spectra were obtained starting at the 1.4 s time delay and then every 3 s for a total of 34 spectra per run. The data were exported to Microsoft Excel and Igor Pro 5.0 for analysis. Plots were made of absorbance versus time for specific wavelengths related to the product, substrate, or heme. The time courses were fit to an exponential fitting function to determine the number of elementary processes that could possibly account for the data. The exponential equation used for nonlinear least-squares fitting is

$$S(t) = A_1 \exp(-k_1 t) + A_2 \exp(-k_2 t) + A_3 \exp(-k_3 t) + B \quad (1)$$

The rate constants are reported in separate tables for each substrate. Depending on the number of components, from one to three rate constants are reported in the tables. Most of the TBP assay spectra fit to double exponentials as shown in Tables 1 and 2.

Enzyme kinetics of DHP and the Y38F mutant were fit using the following expression

$$k = \frac{k_{cat}[TBP]}{K_M + [TBP]} \quad (2)$$

where k is the initial rate constant in units of μM product/μM enzyme/s (also expressed simply as s^{-1}), and k_{cat} is the catalytic rate constant. This expression has a resemblance to Michaelis−Menton enzyme kinetics. However, as discussed elsewhere (*1*, *48*), the complete kinetic expression also includes a dependence on H_2O_2 concentration. In the present study, a kinetic comparison of DHP and Y38F was carried out at a fixed concentration $[H_2O_2] = 1000$ μM and variable TBP concentration from 25 to 600 μM. In control experiments, it was determined that the enzymatic rate, V, is linear in enzyme concentration, $V = k[E]$, where E is the enzyme concentration.

RESULTS

Comparisons of wild-type DHP with the mutants Y38F, H55V, H55V/V59H, H55R and H89G were performed using a spectrophotometric assay, which has sufficient time resolution to determine the relative reactivity at pH 7. Figure 2 shows a comparison of the data for wild-type DHP with Y38F and H55R mutants when TBP is used as the substrate. The substrate TBP has absorption bands at 316 and 249 nm. In the experiments performed here, the disappearance of the TBP substrate is monitored at 316 nm, and the appearance of the product, DBQ, is monitored at 290 nm. Figure 3 shows the time course for the corresponding kinetics at two wavelengths. The number of turnovers in the presence of H_2O_2 can be estimated from the concentration of the product, which is proportional to ΔA at λ_{max} for the product. For wild-type DHP, $\Delta A_{290\ nm}$ is ~0.085 at 1000 s. The extinction coefficient of the product DBQ is 14 000 M^{-1} cm^{-1} so that the concentration of DBQ is ~6 μM. For a DHP concentration of 0.5 μM, the number of turnovers is ~12.

We can generally compare the enzymatic rate using parameters from single or biexponential fits that are given in Table 1. On the basis of the fitting to the rate constants, Y38F has a turnover rate that is ~5 times faster than that of DHP. A more accurate estimate of the enzymatic rate constant was obtained by comparing Y38F's and DHP's initial rates as a function of TBP concentration as shown in Figure 4. The data in Figure 4 and the fits to eq 2 give k_{cat} values of 6.1 ± 1.0 and 1.8 ± 0.5 for Y38F and DHP, respectively. Thus, the enzymatic rate constant k_{cat} is 3.4 times faster for Y38F than for DHP on the basis of the initial rate estimate. The fit values of the constant K_M are 328 ± 111 and 1039 ± 180, respectively. K_M, which is the analogue of the Michaelis constant in the analysis of peroxidase kinetics, is ~3 times smaller for Y38F than that for DHP. The uncertainty in the fit to the wild type data is relatively large because it was not possible to measure rates at saturating values of the substrate because of the high absorbance of both the substrate and the product above [TBP] = 600 μM. On the basis of the k_{obs} value in Table 1, the turnover of the H55R mutant is ~10 times slower than that of the wild type, which is approximately as rapid as the turnover of SWMb. As shown in Figure 5, the remaining mutants H55V, H55V/V59H, and H89G are still less active. It is difficult to compare the kinetics of the less active mutants given the small change in absorbance, and therefore, the

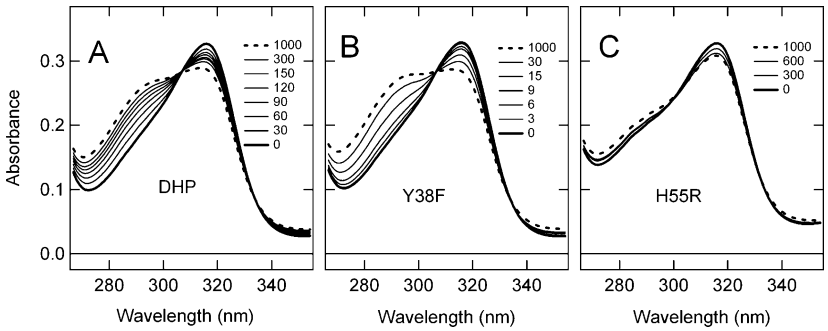

FIGURE 2: Time-dependent spectra for the turnover of TBP by DHP and two mutants, Y38F and H55R, obtained using a photodiode array spectrophotometer. Assay conditions are 0.5 μM enzyme, 50 μM H_2O_2, and 156 μM TBP at pH 7.

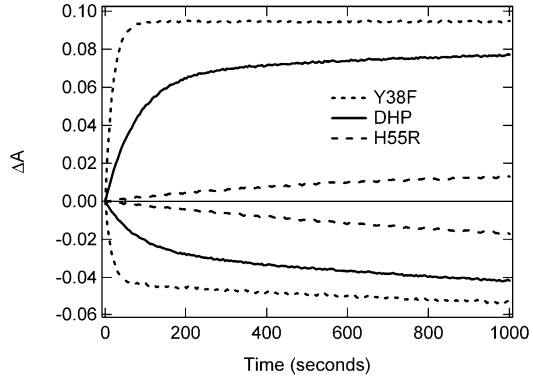

FIGURE 3: Comparison of the time course for the appearance of the DBQ product at 290 nm and the disappearance of the TBP substrate at 316 nm for three different enzymes, DHP wild type, DHP (Y38F), and DHP (H55R). Assay conditions are those given in Figure 2, and the time courses correspond to the time-dependent spectra in that Figure.

analysis of K_M was not performed. For this reason, the relative reactivity of the histidine mutants is compared in Figure 6 by means of the difference in absorption of initial and 1000 s time points. It is clear from Figure 6 that H89G and H55V/V59H have approximately one-half the activity of H55R. The activity of the H55V mutant is further reduced by at least 1 order of magnitude relative to that of H55R.

Figure 7 shows the results of the assay with TCP as the substrate. The peaks of TCP (substrate) and DCQ (product) are observed at 316 and 272 nm, respectively. Figure 8 shows that the same trends in kinetics are observed for the mutant DHP proteins acting on TCP. Y38F has a greater overall yield for the conversion of the TCP substrate to the DCQ product (at least initially), and the H55V, H55V/V59H, and H89G mutants show correspondingly less activity analogous to the trends observed for TBP (data not shown). Figure 8 shows that the activity of H55R toward the oxidation of TCP is significantly reduced relative to that in the DHP wild type. The lack of an increase in absorbance at 272 nm, which is λ_{max} of DCQ, suggests that the consumption of the substrate may result in a one-electron oxidation product that polymerizes (*49*, *50*).

The spectral changes in the heme Soret band associated with activation by H_2O_2 with no added substrate are presented in Figure 9 for DHP and the mutants Y38F and H55R. The Soret band positions are λ_{max} = 407, 414, and 420 nm for the ferric resting state (Fe(III)), oxyferrous form (Fe(II)-O_2), and compound II (Fe(IV)=O), respectively. DHP and Y38F show very similar kinetics. In both species, compound II is formed immediately upon the addition of H_2O_2, and then there is a slow shift of the Soret band from 420 to 414 nm with a decrease in intensity due to suicide inhibition by H_2O_2 followed by the degradation of the heme. At the earliest times, the Soret band spectrum is peaked at 420 nm (compound II) as was also observed by stopped-flow measurements (*1*). Stopped-flow measurements also show that compound I is formed transiently on the time scale of a few seconds (*1*); however, compound I is not observed on the time scale of the experiments reported here. H55R behaves differently. Compound II is never observed in this mutant. Instead, there is a slow shift of the Soret band from 407 to 414 nm with a concomitant decrease in intensity. Table 3 shows the rate constant for the decrease in intensity at the respective λ_{max} values for the different proteins. The

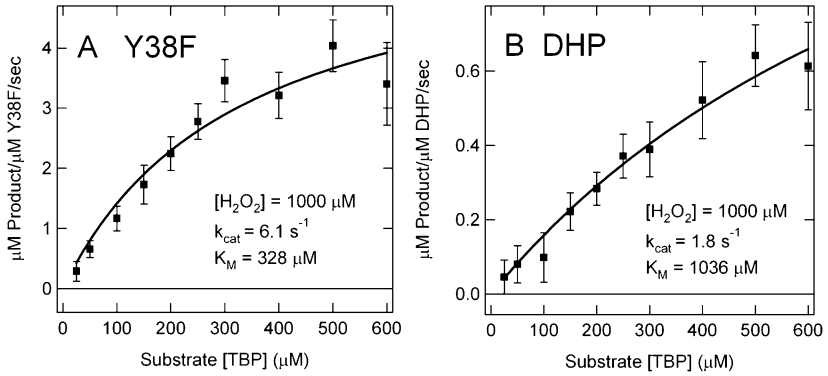

FIGURE 4: Comparison of the enzyme kinetics of wild-type DHP and the Y38F mutant. The initial rate constant was estimated by fitting a linear portion of the first 10 s of the enzyme kinetics of the type shown in Figure 3. To optimize the signal, the enzyme concentrations used in the study were [Y38F] = 0.9 μM and [DHP] = 2.7 μM. The rate constant has units of μM product/μM enzyme/s or simply s^{-1} as indicated in the figure. The data were fit to eq 2.

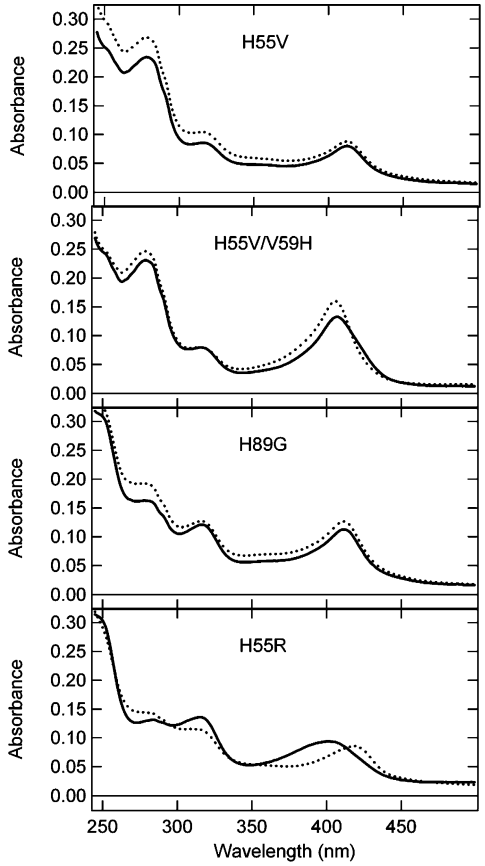

FIGURE 5: Spectra for four mutants shown at the initial and final (1000 s) time points obtained using a photodiode array spectrophotometer. Assay conditions are 0.5 μM enzyme, 50 μM H_2O_2, and 156 μM TBP at pH 7.

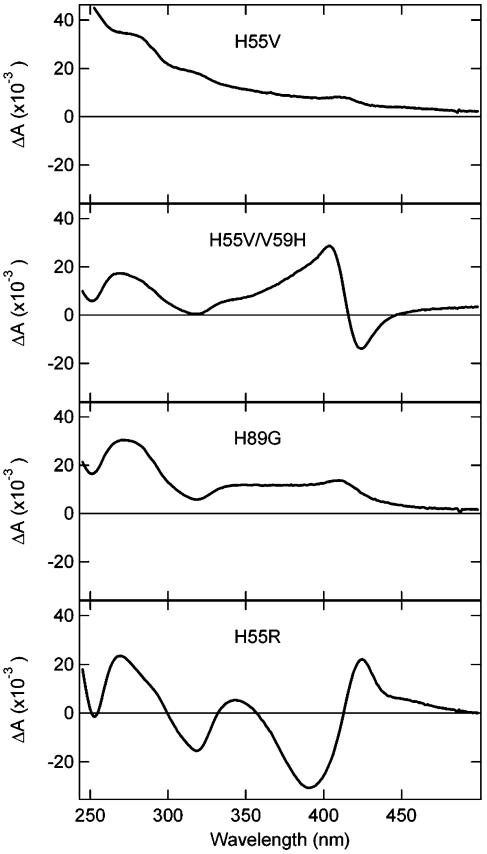

FIGURE 6: Difference spectra for four mutants shown at the initial and final (1000 s) time points obtained using a photodiode array spectrophotometer. Assay conditions are 0.5 μM enzyme, 50 μM H_2O_2, and 156 μM TBP at pH 7.

Table 3: Fits to the Kinetics of the Heme Absorbance of DHP and the Mutants Y38F and H55R at the Absorption Maximum of the Soret Band Following Activation by H_2O_2

enzyme	substrate	λ_{max} (nm)	k_{obs}	ΔA
H55R	none	407	0.00231	0.22 (68%)
			0.00822	0.10 (32%)
DHP	none	420	0.000993	0.19 (43%)
			0.00931	0.25 (57%)
Y38F	none	420	0.00177	0.24 (65%)
			0.00941	0.13 (35%)

kinetic traces are shown in Figure 10. In Figure 9, the similarity of Y38F to the wild type is again evident, whereas H55R shows a different behavior.

The spectral changes in the Soret band when the TBP substrate and H_2O_2 are both added to the DHP enzyme and the two mutants (Y38F and H55R) are shown in Figure 11. The shift from λ_{max} ~407 nm (ferric resting state) to λ_{max} ~420 nm (compound II) is evident in the wild type but not in the mutants. In the case of Y38F, this lack of a shift may arise from a greater enzymatic rate, which results in a low compound II concentration at steady state. In the case of H55R, there appears to be a shift from λ_{max} ~407 nm (ferric resting state) to λ_{max} ~414 nm (oxyferrous form). Under the conditions studied here, there is little decrease in intensity of the Soret band when the substrate is present. The major change is associated with a shift in the Soret band. Regardless of the starting state (ferric or compound II) or the presence of the substrate, the final state of the protein appears to be the oxyferrous form, which is also known as compound III in the peroxidase literature (*51*−*54*).

DISCUSSION

The DHP mutants created and studied here represent structural changes that have precedence in CcP and Mb (*20*−*26*, *31*, *40*, *55*). The mutated amino acids studied here are the distal histidine (H55), the distal valine (V59), the distal substrate-hydrogen-bonded tyrosine (Y38), and the proximal histidine (H89). The distal histidine (H55) plays a key role in the activation of bound peroxide in a peroxidase mechanism. This has been described as the Poulos−Kraut mechanism in a generalized acid−base activation of H_2O_2 to form compound I (*13*, *56*). The distal histidine is the key amino acid residue required for the activation of H_2O_2 to form compound I (*38*). Because H55 is observed in two conformations in the DHP X-ray crystal structure, it is clear that changes in the conformation of H55 are also key for substrate binding (*3*, *4*). Moreover, the obligatory order of substrate binding prior to H_2O_2 binding implies that H55 is in the solvent-exposed position during enzyme activation (*1*). The mutation H55R converts the distal histidine to an arginine with a sufficiently high pK_a such that it would be protonated at pH 7, presumably forcing it into the solvent-exposed or open conformation (Figure 1B). The results show that H55R has significantly reduced activity, but it is still as active as SWMb (*1*). However, H55V replaces the crucial histidine with a valine that likely remains in the distal pocket and may prevent substrate binding or interfere with H_2O_2

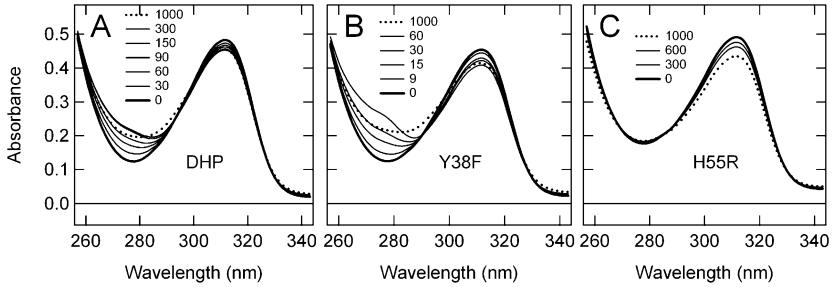

FIGURE 7: Time-dependent spectra for the turnover of TCP by DHP and three mutants Y38F, H55R, and H89G obtained using a photodiode array spectrophotometer. Assay conditions are 0.5 μM enzyme, 50 μM H_2O_2, and 156 μM TCP at pH 7.

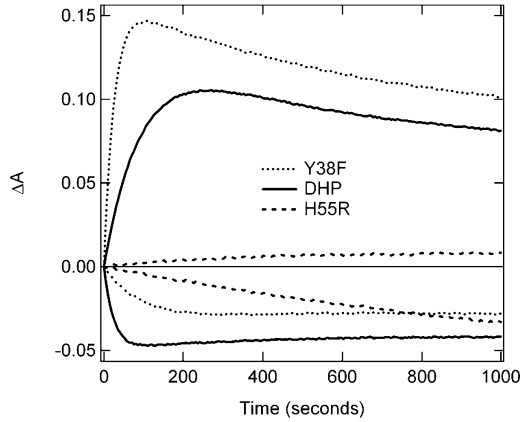

FIGURE 8: Comparison of the time course for the appearance of the DCQ product at 272 nm and the disappearance of the TCP substrate at 316 nm for three different enzymes, DHP wild type, DHP (Y38F), DHP (H55R). Assay conditions are those given in Figure 6, and the time courses correspond to the time-dependent spectra in that Figure.

activation. The H55V mutant shows essentially no activity in accord with this reasoning. The double mutant H55V/V59H tests whether a histidine in position 59 can rescue peroxidase function. Indeed, some residual activity is restored by adding a histidine in the 59 position.

We turn to a more detailed consideration of the role of the distal histidine in DHP. The reduction in activity upon the mutation of the distal histidine was anticipated on the basis of the key role that the distal histidine plays in all known peroxidases. X-ray crystal structures of lignin peroxidase (LiP) (*56*), HRP (*26*), and CcP (*6*, *24*) and their mutants have confirmed the structural basis for the role of the distal histidine in the activation of peroxidases. Figure 1B shows that H55 can exist in a closed conformation in the distal pocket and an open conformation exposed to the solvent (*3*, *4*). Although the histidine is displaced approximately 1.5 Å further from the heme than that in Mb and is observed at a distance of ~6 Å from the heme iron, it is not clear that H55 can play the same role as that of the distal histidine in peroxidases. One reason is that the DHP X-ray structure with 4-iodophenol, a substrate analogue, in the substrate-binding pocket (1EWA) reveals that H55 is ~9 Å from the heme iron when the substrate is present. In the open (substrate bound) conformation, H55 is too far removed from the active site to be involved in the catalysis of the heterolytic bond cleavage of H_2O_2 to yield compound I. To resolve this conundrum, one possible hypothesis is that H55 can effect acid−base catalytic activation of H_2O_2 in DHP prior to substrate binding. However, it was shown by

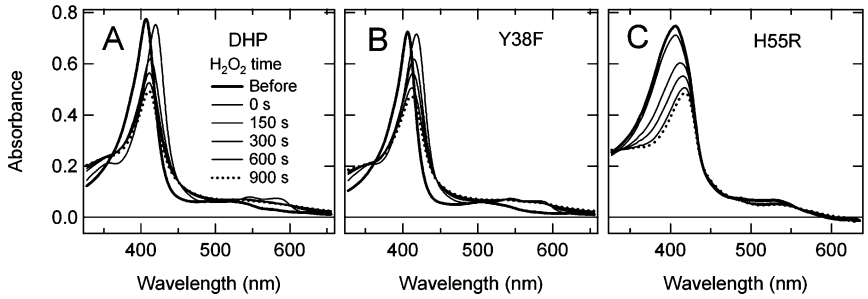

FIGURE 9: Time-dependent spectra for DHP and the Y38F and H55R mutants upon activation by H_2O_2 with no added substrate. Assay conditions are 5 μM DHP and 500 μM H_2O_2 and 100 mM phosphate buffer at pH 7. The time-dependent spectra are given in seconds following H_2O_2 addition.

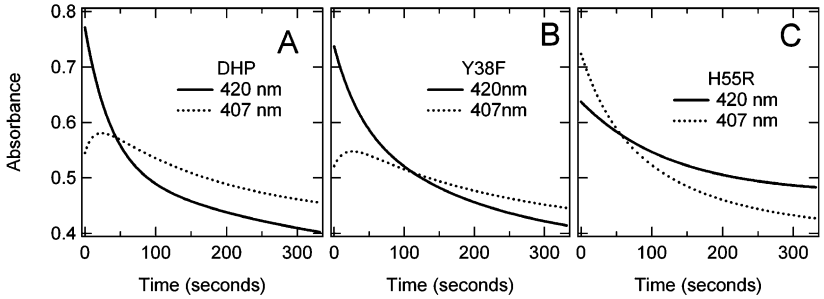

FIGURE 10: Kinetic traces at 407 and 420 nm for DHP and the Y38F and H55R mutants upon activation by H_2O_2 with no added substrate. Assay conditions are 5 μM DHP and 500 μM H_2O_2 and 100 mM phosphate buffer at pH 7.

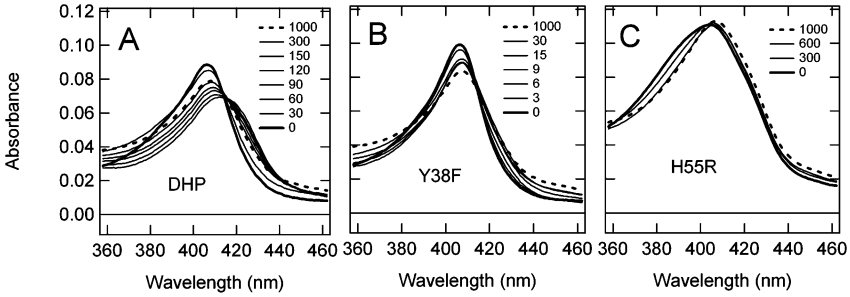

FIGURE 11: Time-dependent changes of the Soret band region of DHP and the mutants Y38F and H55R obtained using a photodiode array spectrophotometer. Assay conditions are 0.5 μM enzyme, 50 μM H_2O_2, and 156 μM TBP at pH 7.

stopped-flow measurements that H_2O_2 binding to the heme iron prior to substrate binding inhibits the enzyme (*1*). These results suggest that the mechanism of DHP does not involve a preactivation of the H_2O_2 cosubstrate prior to substrate binding as observed in other heme peroxidases. The fact that the mutation H55R has a relatively modest effect on enzymatic turnover suggests that H55 does not play the same role as that in the general acid−base model in the Poulos-Kraut mechanism. Rather, it may play the role of a proton shuttle for the substrate and H_2O_2, once both are bound in the distal pocket.

The proximal histidine H89 must support high oxidation states of the heme iron in the peroxidase mechanism. The proximal pocket of CcP (and, therefore, other peroxidases such as LiP and HRP) is highly polarized by the presence of a buried negative charge of an aspartate (or glutamate). The strong hydrogen bonding of Asp to His provides a charge relay that increases the basicity of the proximal ligand (*57*, *58*). This can be written as follows: R-COO$^-$···(δ^+)H-Im(δ^-)···Fe, where δ^+ and δ^- represent the charge displacement that gives rise to an induced dipole on the imidazole. The increase in negative charge at Nϵ increases the lone pair charge density that interacts with the heme iron. This interaction in turn permits the iron to exist in higher oxidation states than is possible in Mb. The mutation of the proximal ligand H89 to glycine produces a DHP protein that has less activity than H55R. Although the structure has not been determined in DHP, it is clear that the H89 mutation is analogous to this mutation, and its activity will have mechanistic implications. H89G is most closely analogous to the proximal cavity mutant H93G of SWMb (*44*, *45*). The H89G mutation has significantly reduced peroxidase activity (even lower than that in Mb), consistent with the observations of the analogous mutation in CcP. The corresponding mutation (H175G) in CcP (*41*) dramatically reduces the activity of the enzyme because the polarization of the proximal pocket requires exogenous imidazole to be bound in the cationic form with phosphate ligated to the heme iron (*42*). Because of the buried negative charge in CcP, it has been observed that imidazole will only enter the proximal pocket as imidazolium, accounting for the reduction in enzymatic activity by 5 orders of magnitude.

The H55R mutation is less active by a factor of ~20 compared to that in the wild type, which is much smaller than the reduction in activity observed in the H175G mutant of CcP. One explanation for the difference in function is found in the DHP X-ray structure that shows a strong hydrogen bond from the proximal histidine in DHP to a neutral moiety and a backbone carbonyl, that is, R-C=O···H-Im···Fe (*3*, *4*). The polarity of the proximal pocket in DHP is much smaller than in CcP. However, the strong hydrogen bond does result in a greater degree of polarization of the heme intermediate between Mbs and peroxidases (*58*). Resonance Raman spectroscopy is consistent with a ligation strength in DHP intermediate between those of Mb and HRP (*2*, *59*). The H89G mutation demonstrates that the geometry of the imidazole in the proximal pocket of DHP is important for catalysis.

The Y38F mutation of DHP was inspired by the mutation Y96F in $P450_{cam}$ (*31*, *60*, *61*). The amino acid Y38 is observed to be hydrogen bonded to the substrate in the X-ray crystal structure of DHP (*3*, *4*), just as camphor is hydrogen bonded to Y96 in $P450_{cam}$ (*62*). The removal of this hydrogen bond in $P450_{cam}$ alters the enantiomeric selectivity toward camphor (*60*), decreases the specificity (*31*), and enhances the activity toward non-native substrates such as styrene (*61*). With such a clear analogy in a monooxygenase, it is obvious that a test of the role of Y38 is an important functional test in DHP.

The most surprising result in the present study is the observation that the Y38F mutant has a more rapid turnover than the wild type. In this regard, Y38F more closely resembles HRP. The decrease in the DBQ product band at 290 nm that is observed in both HRP and Y38F (Supporting Information) is likely due to the presence of a radical pathway that leads to polymerization (*48*−*50*). To understand this point, we consider the following mechanistic scheme applied to DHP. The three steps in the two-electron oxidation mechanism are presented below (*48*)

$$\text{DHP} + \text{H}_2\text{O}_2 \rightarrow \text{compound I} + \text{H}_2\text{O} \qquad (k_1)$$

$$\text{compound I} + \text{XA-OH} \rightarrow \text{compound II} + \text{XA-O}^\bullet + \text{H}^+ \qquad (k_2)$$

$$\text{compound II} + \text{XA-O}^\bullet + \text{H}^+ \rightarrow \text{DHP} + \text{A=O} + \text{HX} \qquad (k_3)$$

where the substrate is XA-OH (X represents the para-halogen and A-OH represents a substituted phenol). Each of these processes is considered to be irreversible. There is a competing pathway that can occur when the substrate concentration is sufficiently high. If the intermediate XA-O$^\bullet$ escapes from the DHP binding site after step 2 or if an edge pathway for electron transfer (*63*) becomes accessible, then a polymerization reaction can occur (*49*, *50*).

$$\text{X(A-O)}_n^\bullet + \text{XA-OH} \rightarrow \text{X(A-O)}_n\text{-A=O}^\bullet + \text{HX}$$

This competing pathway produces an insoluble polymeric product. Because the mechanism of HRP involves two sequential one-electron oxidations that occur at the heme edge (*33*, *63*, *64*), the yield for radicals can be quite high. Phenoxy radicals can polymerize, but they can also react with the product, which is likely responsible for the reduction in intensity at 290 nm observed at times longer than ~100 s in the data shown in Figure 8. The fact that the Y38F mutant shows a similar behavior may be the result of a more rapid substrate off-rate in Y38F relative to that in the wild type for both the product and the intermediate. The net effect is that the reactivity of the heme toward the substrate in the binding pocket more closely resembles the heme-edge electron transfer observed in HRP.

The difference between Y38F and DHP can also be discussed in terms of the ratio k_{cat}/K_M, which gives a measure of the substrate specificity of a heme enzyme. From the fit to the data in Figure 7, it can be seen that k_{cat}/K_M is larger by ~11 for Y38F than for DHP. In other words, not only is the turnover of Y38F more rapid than that of DHP but also the substrate binding is more specific. This is a surprising conclusion given the presence of a hydrogen bond between Y38 and the hydroxyl group of bound phenolic substrate seen in the X-ray crystal structure (*3*). One explanation for this anomalous behavior is that the quinone product may also be strongly hydrogen bonded to Y38, and product release is adversely affected. This explanation leads to the hypothesis that Y38 is present mainly because of the globin function of DHP. It is likely that the globin function is more important to the survival of *A. ornata* than the peroxidase function, and Y38 may play a role in preventing autoxidation or inhibition by other substrates that could enter the binding pocket. A second possible explanation is that the substrate used for these studies (TBP) is not the native substrate.

Suicide inhibition of the heme in peroxidases is prevented by the formation of compound III or by a catalase pathway (*38*, *65*). Ultimately, irreversible reactions may occur, such as the formation of radicals in amino acid side chains or the heme itself. Such reactions are commonly observed in Mb (*34*, *66*, *67*). Thus, it is interesting to compare the globin DHP to HRP to ascertain whether the heme is protected by compound III and catalase pathways. Compound III would be indicated by the presence of a 414 nm heme Soret band in DHP. Catalase activity would give rise to the ferric resting state with a Soret absorption at 407 nm. The time-dependent spectra indicate that there is a substrate dependent shift to 414 nm and a concomitant decrease in the absorbance of the heme Soret band under the conditions used in the present study, that is, a 100:1 ratio of H_2O_2/DHP. The shift is consistent with the formation of a compound III state, and the decrease in intensity is likely due to an irreversible oxidation of the heme itself. In previous studies with lower buffer capacity, the heme Soret band was observed to decrease to some extent even when a substrate was present. In the present study, we show that when a 100 mM phosphate buffer is used, there is little decrease in intensity (degradation of heme) under conditions when a substrate is present, but that significant degradation (probably oxidation) of the heme occurs when no substrate is added. In addition to degradation, there can also be deactivation. The formation of compound III is usually interpreted as the formation of an inactive peroxidase active site. Because DHP is a globin, which has an oxyferrous or compound III resting state, the formation of compound III may have another significance.

In DHP, there is a unique source of inhibition not found in other peroxidases. We have shown in an earlier study that compound II is not a catalytically active species in DHP (*1*). Our current hypothesis for this observation is that native DHP oxidizes halophenols by a two-electron mechanism with the substrate bound in an internal binding pocket (*3*, *4*). On the basis of stopped-flow studies in which the order of the addition of H_2O_2 and TBP is changed, it has been shown that compound II is not capable of oxidizing TBP (*1*). If DHP returned to the resting state (catalase activity), then the enzyme could be regenerated, but there is no spectroscopic evidence that this occurs to a significant extent. In fact, there are only two heme species observed in the Soret band region in the spectra. First, compound II is observed at the shortest possible times (<15 s). This observation is consistent with stopped-flow data where compound II is observed within the mixing time of the stopped-flow apparatus (~2 ms). Then, during the course of the reaction and over a period of minutes, compound III is generated in DHP.

CONCLUSIONS

In the present study, four amino acids in DHP have been mutated to elucidate the enzymatic mechanism in comparison to that of other peroxidases. The mutation of either the distal (H55R, H55V, or H55V/V59H) or the proximal histidine (H89G) results in a significant decrease in activity. Dehaloperoxidase is completely inactivated by the H55V mutation but not by the H55R mutation. This difference is particularly interesting because stopped-flow experiments show that the order of substrate and H_2O_2 binding is critical for enzyme function (*1*). The X-ray structure shows H55 in the solvent-exposed conformation when the substrate is bound suggesting that the distal histidine cannot play the same role in DHP that it plays in other heme peroxidases (*3*, *4*). Although, arginine has a much higher pK_a value than histidine and is protonated under the conditions used in the present measurements, there is still ~16% of native function in the H55R mutant, suggesting that a solvent-exposed distal amino acid can play an important catalytic role. These results suggest that the distal histidine plays the role of a proton shuttle rather than an acid−base catalyst. These observations further substantiate the findings that the distal pocket of DHP and the method of activation of bound H_2O_2 are radically different from other known heme peroxidases. The present study further indicates that the substrate-binding site in DHP is a unique feature of the enzyme. Given the dual function of DHP, the binding site must satisfy the requirements of both globin and peroxidase functions. If substrate binding is a trigger for a switch from a globin to a peroxidase function, then the protein must have evolved to prevent false signals due to the binding of other aromatic molecules. Further experiments will test the role of substrate binding and the key role of residue Y38, which forms a hydrogen bond with the phenol hydroxyl in the substrate-binding pocket.

SUPPORTING INFORMATION AVAILABLE

Singular value decomposition analysis of data and comparison of data in the published M.S. Thesis of Chelsea

Chaudhary (*68*) are presented for comparison. This material is available free of charge via the Internet at http://pubs.acs.org.

REFERENCES

1. Belyea, J., Gilvey, L. B., Davis, M. F., Godek, M., Sit, T. L., Lommel, S. A., and Franzen, S. (2005) The enzyme function of the globin dehaloperoxidase from *Amphitrite ornata* is activated by substrate binding, *Biochemistry 44*, 15637−15644.
2. Franzen, S., Roach, M. P., Chen, Y. P., Dyer, R. B., Woodruff, W. H., and Dawson, J. H. (1998) The unusual reactivities of *Amphitrite ornata* dehaloperoxidase and *Notomastus lobatus* chloroperoxidase do not arise from a histidine imidazolate proximal heme iron ligand, *J. Am. Chem. Soc. 120*, 4658−4661.
3. LaCount, M. W., Zhang, E. L., Chen, Y. P., Han, K. P., Whitton, M. M., Lincoln, D. E., Woodin, S. A., and Lebioda, L. (2000) The crystal structure and amino acid sequence of dehaloperoxidase from *Amphitrite ornata* indicate common ancestry with globins, *J. Biol. Chem. 275*, 18712−18716.
4. Lebioda, L., LaCount, M. W., Zhang, E., Chen, Y. P., Han, K., Whitton, M. M., Lincoln, D. E., and Woodin, S. A. (1999) An enzymatic globin from a marine worm, *Nature 401*, 445.
5. Spiro, T. G., Smulevich, G., and Su, C. (1990) Probing protein structure and dynamics with resonance Raman spectroscopy: Cytochrome *c* peroxidase and hemoglobin, *Biochemistry 29*, 4497−4508.
6. Smulevich, G., Hu, S. Z., Rodgers, K. R., Goodin, D. B., Smith, K. M., and Spiro, T. G. (1996) Heme-protein interactions in cytochrome *c* peroxidase revealed by site-directed mutagenesis and resonance Raman spectra of isotopically labeled hemes, *Biospectroscopy 2*, 365−376.
7. Yamaguchi, K., Watanabe, Y., and Morishima, I. (1992) Push effect on the heterolytic O−O bond cleavage of peroxoiron(II) porphyrin adducts, *Inorg. Chem. 31*, 156−157.
8. Nienhaus, K., Olson, J. S., Franzen, S., and Nienhaus, G. U. (2005) The origin of stark splitting in the initial photoproduct state of MbCO, *J. Am. Chem. Soc. 127*, 40−41.
9. Phillips, G. N., Jr., Teodoro, M. L., Li, T., Smith, B., and Olson, J. S. (1999) Bound CO is a molecular probe of the electrostatic potential in the distal pocket of myoglobin, *J. Phys. Chem. B 103*, 8817−8829.
10. Bonagura, C. A., Bhaskar, B., Shimizu, H., Li, H. Y., Sundaramoorthy, M., McRee, D. E., Goodin, D. B., and Poulos, T. L. (2003) High-resolution crystal structures and spectroscopy of native and compound I cytochrome *c* peroxidase, *Biochemistry 42*, 5600−5608.
11. Blair-Johnson, M., Fiedler, T., and Fenna, R. (2001) Human myeloperoxidase: Structure of a cyanide complex and its interaction with bromide and thiocyanate substrates at 1.9 angstrom resolution, *Biochemistry 40*, 13990−13997.
12. Henriksen, A., Smith, A. T., and Gajhede, M. (1999) The structures of the horseradish peroxidase C-ferulic acid complex and the ternary complex with cyanide suggest how peroxidases oxidize small phenolic substrates, *J. Biol. Chem. 274*, 35005−35011.
13. Poulos, T. L., and Kraut, J. (1980) The stereochemistry of peroxidase catalysis, *J. Biol. Chem. 255*, 8199−8205.
14. Hiner, A. N. P., Raven, E. L., Thorneley, R. N. F., Garcia-Canovas, F., and Rodriguez-Lopez, J. N. (2002) Mechanisms of compound I formation in heme peroxidases, *J. Inorg. Biochem. 91*, 27−34.
15. Dunford, H. B. (2001) How do enzymes work? Effect of electron circuits on transition state acid dissociation constants, *J. Biol. Inorg. Chem. 6*, 819−822.
16. Matsui, T., Ozaki, S., Liong, E., Phillips, G. N., and Watanabe, Y. (1999) Effects of the location of distal histidine in the reaction of myoglobin with hydrogen peroxide, *J. Biol. Chem. 274*, 2838−2844.
17. Quillin, M. L., Arduini, R. M., Olson, J. S., and Phillips, G. N. (1993) High-resolution crystal structures of distal histidine mutants of sperm whale myoglobin, *J. Mol. Biol. 234*, 140−155.
18. Ling, J. H., Li, T. S., Olson, J. S., and Bocian, D. F. (1994) Identification of the iron−carbonyl stretch in distal histidine mutants of carbonmonoxymyoglobin, *BBA Bioenergetics 1188*, 417−421.
19. Balasubramanian, S., Lambright, D. G., and Boxer, S. G. (1993) Perturbations of the distal heme pocket in human myoglobin mutants probed by infrared spectroscopy of bound CO: Correlation with ligand binding kinetics, *Proc. Natl. Acad. Sci. U.S.A. 90*, 4718−4722.
20. Howes, B. D., Rodriguez-Lopez, J. N., Smith, A. T., and Smulevich, G. (1997) Mutation of distal residues of horseradish peroxidase: Influence on substrate binding and cavity properties, *Biochemistry 36*, 1532−1543.
21. Newmyer, S. L., and deMontellano, P. R. O. (1996) Rescue of the catalytic activity of an H42A mutant of horseradish peroxidase by exogenous imidazoles, *J. Biol. Chem. 271*, 14891−14896.
22. Newmyer, S. L., Sun, J., Loehr, T. M., and deMontellano, P. R. O. (1996) Rescue of the horseradish peroxidase His-170 → Ala mutant activity by imidazole: Importance of proximal ligand tethering, *Biochemistry 35*, 12788−12795.
23. Palamakumbura, A. H., Vitello, L. B., and Erman, J. E. (1999) Oxidation of the His-52 → Leu mutant of cytochrome *c* peroxidase by *p*-nitroperoxybenzoic acid: Role of the distal histidine in hydroperoxide activation, *Biochemistry 38*, 15653−15658.
24. Bateman, L., Leger, C., Goodin, D. B., and Armstrong, F. A. (2001) A distal histidine mutant (H52Q) of yeast cytochrome *c* peroxidase catalyzes the oxidation of H_2O_2 instead of its reduction, *J. Am. Chem. Soc. 123*, 9260−9263.
25. Meno, K., Jennings, S., Smith, A. T., Henriksen, A., and Gajhede, M. (2002) Structural analysis of the two horseradish peroxidase catalytic residue variants H42E and R38S/H42E: Implications for the catalytic cycle, *Acta Crystallogr., Sect. D 58*, 1803−1812.
26. Tanaka, M., Ishimori, K., Mukai, M., Kitagawa, T., and Morishima, I. (1997) Catalytic activities and structural properties of horseradish peroxidase distal His42 → Glu or Gln mutant, *Biochemistry 36*, 9889−9898.
27. Nienhaus, K., Deng, P., Belyea, J., Franzen, S., and Nienhaus, G. U. (2006) Spectroscopic study of substrate binding to the carbonmonoxy form of dehaloperoxidase from *Amphitrite* ornata, *J. Phys. Chem. B*, in press.
28. Franzen, S., Jasaitis, A., Belyea, J., Brewer, S., Casey, R., MacFarlane IV, A. W., Stanley, R., Vos, M. H., and Martin, J.-L. (2006) NO-heme geminate recombination dynamics in dehaloperoxidase, *J. Phys. Chem. B*, in press.
29. Franzen, S. (2002) An electrostatic model for the frequency shifts in the carbonmonoxy stretching band of myoglobin: Correlation of hydrogen bonding and the Stark tuning rate, *J. Am. Chem. Soc. 124*, 13271−13281.
30. Yang, F., and Phillips, G. N., Jr. (1996) Crystal structures of CO-, deoxy- and met-myoglobins at various pH values, *J. Mol. Biol. 256*, 762−774.
31. Atkins, W. M., and Sligar, S. G. (1989) Molecular recognition in cytochrome P-450: Alteration of regioselective alkane hydroxylation via protein engineering, *J. Am. Chem. Soc. 111*, 2715−2717.
32. Osborne, R. L., Taylor, L. O., Han, K. P., Ely, B., and Dawson, J. H. (2004) *Amphitrite ornata* dehaloperoxidase: enhanced activity for the catalytically active globin using MCPBA, *Biochem. Biophys. Res. Comm. 324*, 1194−1198.
33. Dunford, H. B. (1995) One-electron oxidations by peroxidases, *Xenobiotica 25*, 725−733.
34. Matsui, T., Ozaki, S., and Watanabe, Y. (1997) On the formation and reactivity of compound I of the His-64 myoglobin mutants, *J. Biol. Chem. 272*, 32735−32738.
35. Ikedasaito, M., Hori, H., Andersson, L. A., Prince, R. C., Pickering, I. J., George, G. N., Sanders, C. R., Lutz, R. S., McKelvey, E. J., and Mattera, R. (1992) Coordination structure of the ferric heme iron in engineered distal histidine myoglobin mutants, *J. Biol. Chem. 267*, 22843−22852.
36. Varadarajan, R., Lambright, D. G., and Boxer, S. G. (1989) Electrostatic interactions in wild-type and mutant recombinant human myoglobins, *Biochemistry 28*, 3771−3781.
37. Pin, S., Alpert, B., Cortes, R., Ascone, I., Chiu, M. L., and Sligar, S. G. (1994) The heme iron coordination complex in His64(E7)Tyr recombinant sperm whale myoglobin, *Biochemistry 33*, 11618−11623.
38. Hiner, A. N. P., Hernandez-Ruiz, J., Rodriguez-Lopez, J. N., Arnao, M. B., Varon, R., Garcia-Canovas, F., and Acosta, M. (2001) The inactivation of horseradish peroxidase isoenzyme A2 by hydrogen peroxide: An example of partial resistance due to the formation of a stable enzyme intermediate, *J. Biol. Inorg. Chem. 6*, 504−516.
39. Vitello, L. B., Erman, J. E., Miller, M. A., Wang, J., and Kraut, J. (1993) Effect of arginine-48 replacement on the reaction between cytochrome *c* peroxidase and hydrogen peroxide, *Biochemistry 32*, 9807−9818.

40. Sun, J., Fitzgerald, M. M., Goodin, D. B., and Loehr, T. M. (1997) Solution and crystal structures of the H175G mutant of cytochrome *c* peroxidase: A resonance Raman study, *J. Am. Chem. Soc. 119*, 2064−2065.
41. McRee, D. E., Jensen, G. M., Fitzgerald, M. M., Siegel, H. A., and Goodin, D. B. (1994) Construction of a bisaquo heme enzyme and binding by exogenous ligands, *Proc. Nat. Acad. Sci. U.S.A. 91*, 12847−12851.
42. Hirst, J., Wilcox, S. K., Williams, P. A., Blankenship, J., McRee, D. E., and Goodin, D. B. (2001) Replacement of the axial histidine ligand with imidazole in cytochrome *c* peroxidase. 1. Effects on structure, *Biochemistry 40*, 1265−1273.
43. Liu, K., Williams, J., Lee, H. R., Fitzgerald, M. M., Jensen, G. M., Goodin, D. B., and McDermott, A. E. (1998) Solid-state deuterium NMR of imidazole ligands in cytochrome *c* peroxidase, *J. Am. Chem. Soc. 120*, 10199−10202.
44. Barrick, D. (1994) Replacement of the proximal ligand of sperm whale myoglobin with free imidazole in the mutant His 93−Gly, *Biochemistry 33*, 6546−6554.
45. DePillis, G., Decatur, S. M., Barrick, D., and Boxer, S. G. (1994) Functional cavities in proteins: A general method for proximal ligand subsitution in myoglobin, *J. Am. Chem. Soc. 116*, 6981−6982.
46. Franzen, S., Boxer, S. G., Dyer, R. B., and Woodruff, W. H. (2000) Resonance Raman studies of heme axial ligation in H93G myoglobin, *J. Phys. Chem. B 104*, 10359−10367.
47. Franzen, S. (2002) Carbonmonoxy rebinding kinetics in H93G myoglobin: Separation of proximal and distal side effects, *J. Phys. Chem. B 106*, 4533−4542.
48. Dunford, H. B. (1999) *Heme Peroxidases*, Wiley-VCH, New York.
49. Harvey, P. J., Floris, R., Lundell, T., Palmer, J. M., Schoemaker, H. E., and Wever, R. (1992) Catalytic mechanisms and regulation of lignin peroxidase, *Biochem. Soc. Trans. 20*, 345−349.
50. Nicell, J. A., Bewtra, J. K., Biswas, N., and Taylor, E. (1993) Reactor development for peroxidase-catalyzed polymerization and precipitation of phenols from waste-water, *Water Res. 27*, 1629−1639.
51. Barr, D. P., and Aust, S. D. (1994) Conversion of lignin peroxidase compound-III to active enzyme by cation radicals, *Arch. Biochem. Biophys. 312*, 511−515.
52. Baynton, K. J., Bewtra, J. K., Biswas, N., and Taylor, K. E. (1994) Inactivation of horseradish peroxidase by phenol and hydrogen peroxide: a kinetic investigation, *BBA Prot. Struct. Mol. Enzymol. 1206*, 272−278.
53. Cai, D. Y., and Tien, M. (1992) Kinetic-studies on the formation and decomposition of compound-II and compound-III: Reactions of lignin peroxidase with H_2O_2, *J. Biol. Chem. 267*, 11149−11155.
54. Coulter, E. D., Cheek, J., Ledbetter, A. P., Chang, C. K., and Dawson, J. H. (2000) Preparation and initial characterization of the compound I, II, and III states of iron methylchlorin-reconstituted horseradish peroxidase and myoglobin: Models for key intermediates in iron chlorin enzymes, *Biochem. Biophys. Res. Commun. 279*, 1011−1015.
55. Hirst, J., Wilcox, S. K., Ai, J. Y., Moenne-Loccoz, P., Loehr, T. M., and Goodin, D. B. (2001) Replacement of the axial histidine ligand with imidazole in cytochrome *c* peroxidase. 2. Effects on heme coordination and function, *Biochemistry 40*, 1274−1283.
56. Poulos, T. L., Edwards, S. L., Wariishi, H., and Gold, M. H. (1993) Crystallographic refinement of lignin peroxidase at 2-angstrom, *J. Biol. Chem. 268*, 4429−4440.
57. Goodin, D. B., and McRee, D. E. (1993) The Asp-His-Fe triad of cytochrome *c* peroxidase controls the reduction potential, electronic structure, and coupling of the tryptophan free radical to the heme, *Biochemistry 32*, 3313−3324.
58. Franzen, S. (2001) Effect of a charge relay on the vibrational frequencies of carbonmonoxy iron porphine adducts: The coupling of changes in axial ligand bond strength and porphine core size, *J. Am. Chem. Soc. 123*, 12578−12589.
59. Belyea, J., Lappi, S., and Franzen, S. A Resonant Raman study of the core size marker modes of dehaloperoxidase from *Amphitrite ornata*, *Biochemistry*, submitted for publication.
60. Niaura, G., Reipa, V., Mayhew, M. P., Holden, M., and Vilker, V. L. (2003) Structural alterations of the heme environment of cytochrome P450cam and the Y96F mutant as deduced by resonance Raman spectroscopy, *Arch. Biochem. Biophys. 409*, 102−112.
61. Nickerson, D. P., Harford-Cross, C. F., Fulcher, S. R., and Wong, L.-L. (1997) The catalytic activity of cytochrome P450cam towards styrene oxidation is increased by site-specific mutagenesis, *FEBS Lett. 405*, 153−156.
62. Poulos, T. L., Finzel, B. C., and Howard, A. J. (1987) High-resolution crystal structure of cytochrome P450cam, *J. Mol. Biol. 195*, 687−700.
63. Ator, M. A., and Ortiz de Montellano, P. R. (1987) Protein control of prosthetic heme reactivity reaction of substrates with the heme edge of horseradish peroxidase, *J. Biol. Chem. 262*, 1542−1551.
64. La Mar, G. N., Hernandez, G. and de Ropp, J. S. (1992) Proton NMR investigation of the influence of interaction sites on the dynamics and thermodynamics of substrate and ligand binding to horseradish peroxidase, *Biochemistry 31*, 9158−9168.
65. Arnao, M. B., Acosta, M., Delrio, J. A., Varon, R., and Garcia-Canovas, F. (1990) A kinetic study on the suicide inactivation of peroxidase by hydrogen peroxide, *Biochim. Biophys. Acta 1041*, 43−47.
66. Villegas, J. A., Mauk, A. G., and Vazquez-Duhalt, R. (2000) A cytochrome *c* variant resistant to heme degradation by hydrogen peroxide, *Chem. Biol. 7*, 237−244.
67. Witting, P. K., Mauk, A. G., and Lay, P. A. (2002) Role of tyrosine-103 in myoglobin peroxidase activity: Kinetic and steady-state studies on the reaction of wild-type and variant recombinant human myoglobins with H_2O_2, *Biochemistry 41*, 11495−11503.
68. Chaudhary, C. (2003) M.S. Thesis, North Carolina State University, Raleigh, NC.
69. Vojtechovsky, J., Chu, K., Berendzen, J., Sweet, R. M., and Schlichting, I. (1999) Crystal structures of myoglobin-ligand complexes at near-atomic resolution, *Biophys. J. 77*, 2153−2174.

BI060020Z